Journal Pre-proof

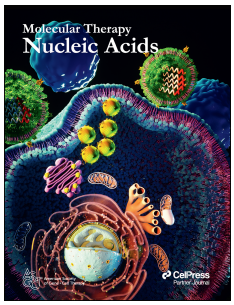

Restoration of functional PAX6 in aniridia patient iPSC-derived ocular tissue models using repurposed nonsense suppression drugs

Dulce Lima Cunha, Hajrah Sarkar, Jonathan Eintracht, Philippa Harding, Jo Huiqing Zhou, Mariya Moosajee

PII: S2162-2531(23)00167-1

DOI: https://doi.org/10.1016/j.omtn.2023.06.016

Reference: OMTN 1953

To appear in: *Molecular Therapy: Nucleic Acid*

Received Date: 26 May 2022

Accepted Date: 22 June 2023

Please cite this article as: Cunha DL, Sarkar H, Eintracht J, Harding P, Zhou JH, Moosajee M, Restoration of functional PAX6 in aniridia patient iPSC-derived ocular tissue models using repurposed nonsense suppression drugs, *Molecular Therapy: Nucleic Acid* (2023), doi: https://doi.org/10.1016/j.omtn.2023.06.016.

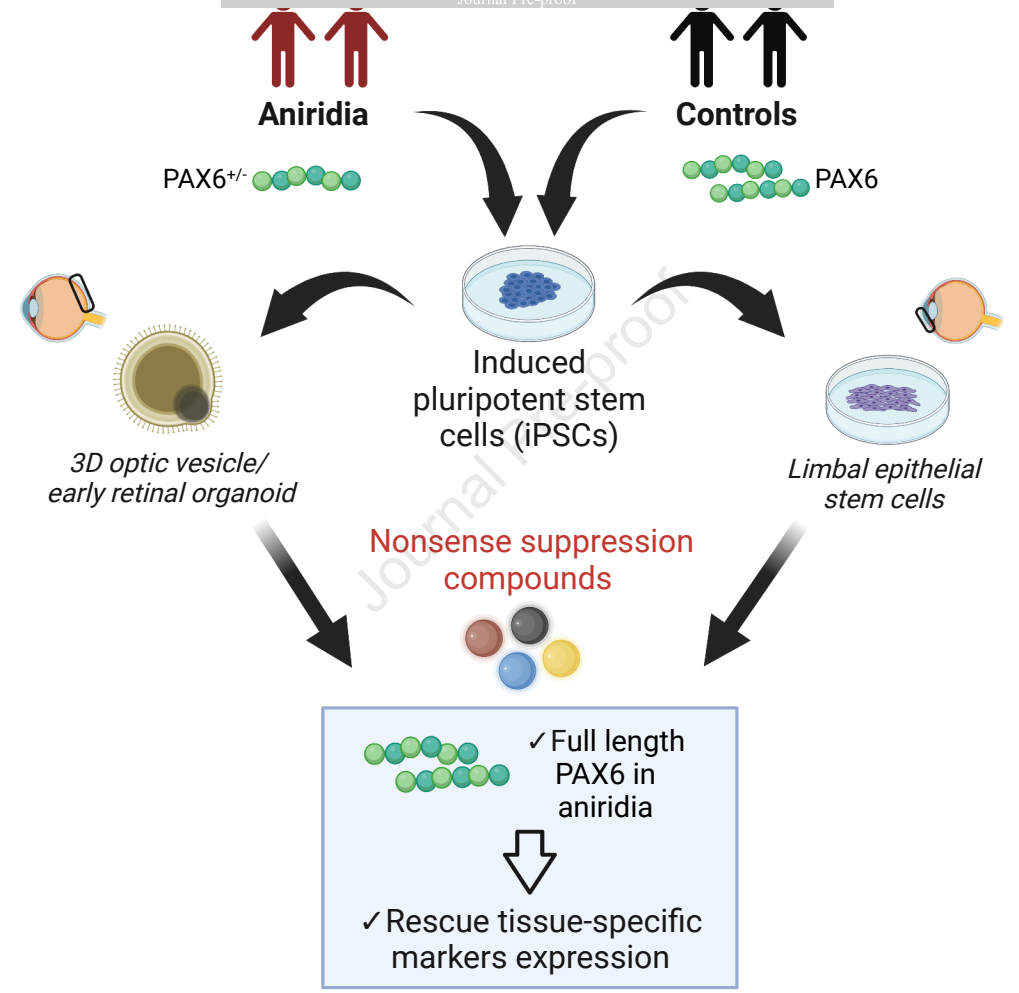

Restoration of functional PAX6 in aniridia patient iPSC-derived ocular tissue models using repurposed nonsense suppression drugs

Authors: Dulce Lima Cunha[1,2], Hajrah Sarkar[1,3], Jonathan Eintracht[1], Philippa Harding[1], Jo Huiqing Zhou[2] and Mariya Moosajee[1,3,4]

1. UCL Institute of Ophthalmology, London, UK
2. Radboud Institute of Molecular Life Sciences, Radboud University, Nijmegen, Netherlands
3. The Francis Crick Institute, London UK
4. Moorfields Eye Hospital, London, UK

Correspondence should be addressed to:
Mariya Moosajee. MBBS BSc PhD FRCOphth
UCL Institute of Ophthalmology
11-43 Bath Street, EC1V 9EL
London, UK
Tlf: +442076086971
Email: m.moosajee@ucl.ac.uk

Short title: PAX6 rescue with novel readthrough compounds

Abstract

Congenital aniridia is a rare, pan-ocular disease causing severe sight loss, with only symptomatic intervention offered to patients. Approximately 40% of aniridia patients present with heterozygous nonsense variants in *PAX6,* resulting in haploinsufficiency. Translational readthrough inducing compounds (TRIDs) have the ability to weaken the recognition of in-frame premature stop codons (PTCs), permitting full-length protein to be translated. We have established induced pluripotent stem cell (iPSC)-derived 3D optic cups and 2D limbal epithelial stem cell (LESC) models from two aniridia patients with prevalent *PAX6* nonsense mutations. Both *in vitro* models show reduced PAX6 protein levels, mimicking the disease. Repurposed TRIDs amlexanox and 2,6-diaminopurine (DAP), and positive control compounds ataluren and G418 were tested for their efficiency. Amlexanox was identified as the most promising TRID, increasing full-length PAX6 levels in both models, and rescuing the disease phenotype through normalization of VSX2 and cell proliferation in the optic cups and reduction of ABCG2 protein and *SOX10* expression in LESC. This study highlights the significance of patient iPSC-derived cells as a new model system for aniridia and proposes amlexanox as a new putative treatment for nonsense-mediated aniridia.

Introduction

Aniridia (OMIM 106210) is a rare, dominant, pan-ocular disease, with a prevalence of 1 in 40,000-100,000 [1]. Typical symptoms of this disease include congenital iris and foveal hypoplasia with nystagmus, and progressive development of glaucoma, cataracts and keratopathy, leading to significant visual impairment [2-4]. Up to 90% of aniridia patients develop limbal stem cell deficiency (LSCD), where adult epithelial stem cells originating in the limbus and maintain corneal transparency, are lost or defective, causing impaired epithelium renewal and conjunctival invasion [5]. LSCD invariably results in complete corneal opacity, usually termed aniridia-related keratopathy (ARK), and is the most relevant feature contributing to visual loss in aniridia post-natally [5,6].

Heterozygous mutations affecting the *PAX6* gene or its regulatory regions are the cause of aniridia [7,8], with mutations introducing a premature stop codon (PTC) being the most common (http://lsdb.hgu.mrc.ac.uk/home.php?select_db=PAX6). Of these, nonsense mutations are the most prevalent, accounting for 39% of the total mutations reported in aniridia patients [9]. *PAX6* nonsense mutations are predicted to result in loss of function, where mutated mRNA is likely degraded by nonsense-mediated decay (NMD), resulting in *PAX6* haploinsufficiency.

Nonsense suppression or translational readthrough inducing compounds (TRIDs) weaken the recognition of a PTC and promote the replacement of a near cognate amino acid, thus allowing translation to continue and producing a full-length protein [10,11]. Promising preclinical data using ataluren (also called Translarna or PTC124), a TRID approved for the treatment of Duchenne muscular atrophy, showed rescue of Pax6 levels in the aniridia *Sey*$^{+/-}$ mouse model, with topical administration inhibiting disease progression and improving corneal, lens, and retinal defects [12,13]. A phase I/II clinical trial (NCT02647359) for aniridia was completed, but failed to meet the primary endpoint, despite showing a positive trend towards functional improvement (https://www.prnewswire.com/news-releases/ptc-therapeutics-reports-fourth-quarter-and-full-year-2019-financial-results-and-provides-a-corporate-update-301014669.html). The use of TRIDs is a particularly suitable therapeutic approach for aniridia due to the high prevalence of nonsense variants and the milder phenotype associated with *PAX6* missense mutations [2,3,9]. However, novel readthrough compounds with improved efficiency are required with a personalized medicine approach, knowing which TRIDs may be more effective for specific PTCs or that combined inhibition of nonsense-mediated decay may boost mRNA substrate and end protein production.

PAX6 is a dose-sensitive transcription factor essential for eye development [7,8]. It is expressed early in ocular morphogenesis, during the establishment of the eye field and optic vesicle, and has multiple roles in the development and maintenance of retinal progenitor cells, lens, cornea and iris

[14]. In the cornea, correct Pax6 levels are required for normal cell growth during limbal and central corneal epithelial development, but the exact mechanisms on how *PAX6* haploinsufficiency causes LSCD and ARK are still not understood [15]. It was recently shown that Pax6 controls neural crest migration during corneal development, a process important for the formation of the non-epithelial corneal layers, i.e. stroma and endothelium, as well as for maintenance of the limbal niche [16-18].

The generation of human induced pluripotent stem cells (iPSCs) has opened a new avenue in establishing representative *in vitro* models that can recapitulate human development and provide valuable insights on disease mechanisms [19]. They have been used to accelerate therapeutic development in several retinal and corneal eye disorders [20-22]. This is the first study to generate iPSCs from aniridia patients carrying heterozygous *PAX6* nonsense mutations, with a UGA-type PTC, and establish patient-specific iPSC-derived optic cups and limbal epithelium stem cell (LESC) models that mimic the haploinsufficiency state. We used these models to assess the potential of TRIDs amlexanox and 2,6-diaminopurine (DAP) to treat aniridia. Amlexanox is a FDA-approved drug used for the treatment of asthma and aphthous mouth ulcers [23], that was found to have both readthrough and NMD-inhibition properties [24-26]; DAP is an antileukemia compound with recently identified strong readthrough capacity for UGA-type PTC [27].

We identified amlexanox as the most promising TRID, increasing full-length PAX6 levels and rescuing phenotype abnormalities in both iPSC-derived retinal and corneal models, while DAP showed distinct tissue dependent responses. Our results provide substantial proof-of-concept for the use of amlexanox as a new therapeutic approach for aniridia.

Results

Generation of aniridia induced pluripotent stem cells (iPSCs)

Human dermal fibroblasts taken from two molecularly confirmed aniridia patients (AN1 and AN2) were reprogrammed into iPSCs by electroporation using non-integrating episomal plasmids [28,29]. Generated iPSC clonal lines were thoroughly and routinely characterized, showing positive

pluripotency markers, tri-lineage differentiation ability and chromosomal stability (Supplementary Figure 1). AN1 patient carries a heterozygous nonsense variant in *PAX6* (NM_000280.4) c.781C>T/ p.(Arg261*), while AN2 patient carries the heterozygous nonsense variant c.607C>T/ p.(Arg203*). Both variants are predicted to introduce a UGA PTC. The disease-causing variants were confirmed in each AN iPSCs by direct sequencing of *PAX6* exons 10 (AN1) and 8 (AN2) (Figure 1A and Supplementary Figure 1A).

Aniridia iPSC-derived optic cups show reduced PAX6 protein but not mRNA levels

AN1-iPSCs as well as two independent iPSC lines derived from unaffected healthy controls (WT1 and WT2) were further differentiated into 3D optic cup-like stage by adapting established protocols [30,31] (Figure 1B). Differentiating organoids showed upregulation of eye field transcription factors (EFTFs) *RAX* and *PAX6* from day 10 onwards (Figure 1C,D) [32,33]. No significant differences in *PAX6* mRNA levels were detected between AN1- and WT(1 and 2) -iPSC-OCs throughout the process, although a downregulation compared to WT seems apparent from day 15 (Figure 1D). RT-PCR of *PAX6* cDNA shows presence of AN1 mutated transcript (Figure 1E), while *UPF1* expression, a key activator of NMD, is unchanged compared to WT1 (Supplementary Figure 2A), suggesting NMD escape. In contrast, PAX6 protein immunoblotting showed significant reduction of PAX6 protein in AN iPSC-OCs at day 35, with approx. 0.33 ± 0.23 fold of WT(1 and 2) levels ($p<0.01$, Figure 1F). Despite the reduced PAX6 protein, AN1 organoids could progress into an optic cup (OC) like stage, typically around differentiation day 35, when both neural retina marker VSX2 (Visual system homeobox 2) and retinal pigmented epithelium (RPE) marker MITF (Microphthalmia-associated transcription factor) are present (Figure 1G). Expression of pluripotency markers *OCT4* and *LIN28* was reduced throughout the differentiation process, showing exit from pluripotency state (Supplementary Figure 3A).

Establishment and characterization of AN iPSCs-derived limbal epithelial stem cells

To test the clinical potential of TRIDs as possible therapy for aniridia limbal stem cell deficiency, we differentiated the two aniridia iPSC lines (AN1 and AN2), together with control lines WT1 and WT2, into 2D limbal epithelial stem cells (LESCs) [34]. A third control, the H9 embryonic stem cell (ESC) line was also included at this stage to limit inter-donor variability often seen in iPSCs[35]. Following formation of embryoid bodies (EBs), limbal fate was induced for 5 days and EBs were plated onto collagen IV coated pates, where epithelial-like cells emerged and proliferated until day 15 (Figure 2A). Timepoint analysis confirmed high expression of LESCs specific markers *ΔNP63α*, *KRT14* and *ABCG2* by day 15 in all AN and WT control lines, proving limbal commitment (Figure 2B); this was also confirmed in the differentiated H9 ESC line (Supplementary Figure 4). In parallel, pluripotency markers *OCT4*, *SOX2* and *LIN28* were downregulated for all lines, showing exit from pluripotency state (Supplementary Figure 3B).

Similar to our 3D optic cup model, no clear differences in *PAX6* mRNA expression were detected between our AN and WT lines (Figure 2C); however, a significant reduction in full length PAX6 protein was seen in both AN1 and AN2 iPSC-LESCs after protein analysis at day 15, with both lines showing approximately one third of PAX6 control levels (AN1: 0.37 ± 0.13 fold; AN2: 0.33 ± 0.14 fold vs WT=1, $p<0.01$) (Figure 2D). NMD activity was assessed through *UPF1* expression, which remained unchanged between the different iPSC (and ESC)-derived LESCs (Supplementary Figure 2B).

Amlexanox and Ataluren increase full-length PAX6 levels in aniridia iPSC-optic cups

To test the potential of TRIDs to increase full length PAX6 levels, AN iPSC-OCs were dosed with readthrough compounds amlexanox and DAP, as well as ataluren and G418 from day 15 until collection on day 35 (Figure 1B). G418 caused cell toxicity, even when lower concentrations were tested; the same scenario was observed after DAP dosing, with no viable cells found after day 20/25 (Supplementary Figure 5). The same occurred when dosing WT iPSC-OCs with both drugs,

pointing towards drug-specific toxicity. In contrast, amlexanox and ataluren were well tolerated, and no major morphological differences in optic-cup structures were found after dosing (Figure 3A).

Full length PAX6 was detected by Western blot in WT, dosed and undosed AN1 iPSC-OC samples on day 35. We observed that 250μM amlexanox treatment increased full length PAX6 levels by nearly 4-fold (1.24 ± 0.31, $p<0.05$) compared to untreated AN1 samples. There was a relative increase in PAX6 in ataluren-treated samples, but it did not reach statistical significance (0.90 ± 0.50, $p= 0.22$) (Figure 3B). Immunostaining confirmed this result, with untreated AN1 showing weaker PAX6 staining in the neural retina layer of untreated AN organoids, which improved after treatment with amlexanox (Figure 3C).

Phenotype rescue in TRID-treated aniridia iPSC-OCs

In order to determine if the increased protein levels following treatment with amlexanox resulted in a functional PAX6 rescue as well as improvement in molecular and cellular phenotype, we investigated the expression of key optic cup marker VSX2. In vivo, VSX2 is necessary for the establishment of retinal progenitor cells (RPCs) in the optic cup and, in the total absence of PAX6, VSX2 expression, along with optic vesicle progression into the optic cup, is abrogated [14]. Interestingly, the AN1 iPSC-OCs showed a 4.08 ± 0.74 fold increase of *VSX2* mRNA levels ($p<0.001$) and immunostaining confirmed a stronger VSX2 signal in untreated AN1 compared to WT iPSC-OCs (Figure 3D,E). After both amlexanox and ataluren treatment, *VSX2* expression was significantly downregulated to 1.02 ± 0.67 ($p<0.001$) and 1.05 ± 0.65 -fold ($p<0.001$), respectively, which was indistinguishable from the levels detected in WT samples (WT expression =1) (Figure 3D). Similarly, immunostaining on day 35 showed weaker VSX2 staining in amlexanox versus untreated AN1 iPSC-OCs. This was less clear for ataluren-treated AN1 iPSC-OCs (Figure 3E).

178 Cell proliferation alterations have been previously reported in response to abnormal *Pax6* levels
179 [36,37]. Indeed, we observed a significant upregulation in *MKI67* expression, which encodes the
180 proliferation marker Ki-67, in AN1 iPSC-OCs compared to WT (1.65 ± 0.26 fold, p<0.01). This
181 increased proliferative status was also fully rescued after dosing with amlexanox (0.99 ± 0.16,
182 p<0.01) and ataluren (1.07±0.28, p<0.05) (Figure 3F).
183
184 ***TRIDs increase PAX6 protein and improve phenotype in iPSC-LESCs***
185 Due to reduced PAX6 protein levels already detected in aniridia iPSC-LESCs at day 15, we dosed
186 cells for 48h, from day 13 until harvest on day 15 [24]. Cells treated with 250 µM amlexanox showed
187 affected viability, so lower concentrations, 100 µM and 200 µM, were used. DAP concentrations of
188 100 µM and 200 µM did not affect cell viability, neither did 40 µM ataluren. In contrast, G418 caused
189 significant cell death in iPSC-LESCs, even at doses lower than 100µg/mL, hence readthrough
190 effect could not be analysed. This was similar to that observed in the 3D optic cup models,
191 confirming G418 cytotoxicity [10,38]. Overall, TRIDs dosing increased full-length PAX6 in AN1 iPSC-
192 LESCs (Figure 4A): amlexanox significantly improved protein levels to 0.650 ± 0.043 -fold (100 µM,
193 p<0.05) and 0.941 ± 0.085-fold (200 µM, p<0.0001). Also 100 µM DAP treatment improved PAX6
194 levels to 0.912 ± 0.064 (p<0.001). Ataluren-treated cells also showed significant increase in PAX6,
195 with full-length levels reaching 0.85±0.048-fold (p<0.001) of control levels (Figure 4A). AN2 iPSC-
196 LESCs showed similar trends of increased PAX6 protein when dosed with TRIDs, but failed to
197 reach significance when treated with ataluren or amlexanox (Figure 5A). However, 100µM DAP
198 treatment lead to the significant increase of full length PAX6 (0.809±0.16-fold, p<0.05) (Figure 5A).
199 Treatment of AN1 and AN2 iPSC-LESCs with drugs vehicle (DMSO) alone showed no significant
200 changes compared to untreated cells (Supplementary Figure 6A,B). Importantly, dosing of control
201 H9 ESC-derived LESCs with the same TRIDs also showed no effect on PAX6 protein levels,

supporting the specificity of these drugs to readthrough of the mutated allele (Supplementary Figure 6C).

To assess for functional and phenotypic rescue following treatment with TRIDs we examined expression of ABCG2, which is transiently expressed in LESCs and is considered a LESC-specific stemness marker [39]. Although the relationship between PAX6 and ABCG2 is not known, it was recently shown that *ABCG2* mRNA is upregulated in LESCs extracted from aniridia patients (with PTC-causing mutations) compared to controls [40]. We observed similar results in our iPSC-derived system, where *ABCG2* mRNA peaked at day 10 in all lines (Figure 2B) and, at day 15, there was a 5.40 ±1.79 fold accumulation of ABCG2 protein in AN1 and 5.49±1.6 fold in AN2 compared to WT control iPSC-LESCs ($p<0.05$) (Figure 4B, 5B). Remarkably, amlexanox-treated AN1 iPSC-LESCs showed a very significant reduction in ABCG2 protein, reaching levels very close to WT, with both concentrations: 100µM (1.70 ± 0.10 -fold, $p<0.05$) and 200µM (1.75 ± 0.59, $p<0.05$) (Figure 4B). Although the same trend was observed for (100 µM) amlexanox-treated AN2 iPSC-LESCs, it did not achieve statistical significance (2.11 ± 1.49-fold, $p=0.08$) (Figure 5B).

SOX9 and SOX10 are TFs expressed in the neural crest-fate cells in the limbal niche, which is essential for the homeostasis of LESCs [17]. Therefore, and because PAX6 was recently shown to drive neural crest migration during corneal development [16,18], we tested the expression of *SOX9* and *SOX10* between AN and WT iPSC-LESCs. Although *SOX9* expression was not significantly altered between AN and WT (Figure 4C, 5C), we found that *SOX10* was sharply upregulated in both AN iPSC-LESCs (AN1: 20 ±1.29 -fold, $p<0.001$, Figure 4D; AN2: 10.31±1.29 -fold, $p<0.001$, Figure 5D). Following treatment with TRIDs, *SOX10* expression was rescued by 100µM and 200µM

of amlexanox, as well as with ataluren in both patient cell lines (Figure 4D, 5D). Similarly to previous results, DAP did not induce an improvement in *SOX10* expression (Figure 4D, 5D).

In conclusion, amlexanox increases full-length PAX6 levels and rescues phenotypic differences in both early 3D optic cups and 2D limbal epithelial stem cells generated from aniridia patients iPSCs, proving that newly synthesized PAX6 is functional and the new amino acid inserted is likely tolerated.

Discussion

The aim of this work is to provide proof of principle for the further development of repurposed readthrough drugs amlexanox and 2,6-diaminopurine (DAP) for aniridia. Aniridia is a highly suitable disease for readthrough therapy approaches, due to the high prevalence of *PAX6* nonsense mutations, dosage sensitivity, and if the target tissue is well considered i.e. cornea and LESC to reduce aniridia-related keratopathy (ARK) and maintain levels of vision. Insufficient PAX6 levels, or haploinsufficiency, is thought to be the underlying genetic mechanism of aniridia; therefore, increasing full-length PAX6 levels, even if not fully, might be enough to attenuate disease. This is also supported in patients, where PTC-introducing variants are generally associated with severe forms of aniridia, whilst patients with missense mutations usually present with milder phenotypes and less severe vision loss [2,3,6].

We generated an iPSC line from an aniridia patient carrying the heterozygous *PAX6* nonsense mutation c.781C>T, p.(Arg261*). This variant is located within the “PAX6 mutation hotspot”, a region in exons 8 to 13 with methylated CpG islands, where 21% of all mutations and 60% of all nonsense mutations are located [9,41,42].

We have differentiated the patient iPSCs into 3D optic cups (iPSC-OCs) and show significantly reduced PAX6 protein levels at day 35, a timepoint comparable to the *in vivo* optic cup stage. Nonetheless, these reduced PAX6 levels are sufficient to form optic cup domains (neural retina

and RPE) in our *in vitro* system, which is also consistent with *in vivo* results [14]. Amlexanox and ataluren were shown to recover levels of full-length PAX6, while DAP and G418 showed toxicity at all concentrations tested.

We observed a striking increase in neural retina marker VSX2 expression in aniridia iPSC-derived optic cups. Low Pax6 levels seem to promote early neurogenesis in the mice optic vesicle [14]; this might explain the accumulation of VSX2, which was detected at both mRNA and protein levels. Importantly, we observe that normal VSX2 levels are restored after treatment of aniridia iPSC-OCs with amlexanox and ataluren. These results suggest that both compounds induce functional PAX6 protein increase, leading to rescue of the *in vitro* phenotype. This was further supported by the downregulation of proliferation marker *MKi67* expression, known to be increased in *Pax6* mutant cells, after dosing of aniridia iPSC-OCs with both TRIDs [36].

The role of PAX6 in the eye is both time- and tissue-specific, acting during development but also on maintenance of adult tissue [14,43]. This translates into a developmental and progressive disease, where aniridia patients typically show hypoplasia of the iris and fovea from birth, and progressive opacity of the lens and cornea from childhood/early adulthood [1,9]. From large natural history studies we understand that the visual acuity remains relatively stable over decades of life [3]. Therapeutic approaches targeting developmental defects are currently not feasible, hence we aimed to test the clinical potential of TRIDs to halt or slow down ARK, which can affect up to 90% patients and is the mainstay for a decline in visual acuity over time [9]. For that purpose, we established a second aniridia human model, by growing patient iPSC-derived 2D limbal epithelial stem cells (iPSC-LESCs). Upregulation of LESCs specific markers *ΔNP63α*, *ABCG2* and *KRT14* in these cells proved commitment to the limbal fate. Aniridia patients iPSC-LESCs show over 60% reduction in PAX6 protein levels, lower than the estimated 50%, validating this model to study *PAX6* haploinsufficiency. Once again, we did not observe significantly reduced *PAX6* transcript levels in AN vs WT iPSC-LESCs during the first 15 days of differentiation. It is assumed that *PAX6* null

278 variants lead to the degradation of the mutated transcripts via NMD, thus resulting in
279 haploinsufficiency [9]; however, we do not seem to observe this in our *in vitro* models; in fact, in the
280 aniridia iPSC-OCs, we could prove the presence of the mutated transcript, pointing to likely NMD
281 escape. NMD is a multifactorial complex mechanism, its variable activity has been documented
282 and can vary between patients with the same mutation, as seen in a study involving X-linked
283 choroideremia patients; four individuals with a c.715 C>T; p.(R239*) UGA mutation displayed *CHM*
284 transcript levels ranging from 13% to 52.6% [44]. In addition, previous studies have shown that NMD
285 efficiency varies between different murine tissues [45], but in the choroideremia study no significant
286 difference in *CHM* mRNA levels were seen between two different patients' fibroblast lines and their
287 corresponding iPSC-derived RPE [44]. The nonsense variants described in this study do result in loss
288 of function and we therefore hypothesize that other mechanisms could contribute to *PAX6*
289 haploinsufficiency, such as post-translational modifications or epigenetic regulations of the
290 protein[46,47], and requires further investigation.
291
292 Dosing of AN1 iPSC-LESCs with different TRIDs resulted in similar profiles compared to 3D optic
293 cups; both amlexanox and ataluren proved to significantly increase PAX6 protein, although slightly
294 lower concentrations of amlexanox were used due to very low proliferation in cells treated with
295 250µM. Importantly, both compounds, but particularly amlexanox, induced strong phenotype
296 rescue by restoring ABCG2 as well as *SOX10* levels, two important players in limbal epithelial stem
297 cell identity and survival, respectively [17,39]. Although DAP also induced a significant increase in
298 PAX6 levels in AN1 (and AN2) iPSC-LESCs, it did not show a significant downstream phenotypic
299 rescue. We hypothesize this is due to the new amino acid introduced, i.e. tryptophan, which may
300 still have a deleterious effect [27]. Ataluren was well tolerated in both models; in contrast, G418 was
301 highly cytotoxic, proving the downside of traditional aminoglycosides use and need for less toxic
302 TRIDs [10]. DAP showed variable toxicity in iPSC-derived OCs versus LESCs from the same patient
303 (AN1), being cytotoxic in the former and well tolerated and efficient in the latter. Its readthrough
304 ability was only very recently reported so its mechanism remains unclear [27]. DAP induced a

significant increase in PAX6 levels in AN iPSC-LESCs, but did not show significant downstream phenotype rescue. We hypothesize this is due to the new amino acid introduced by the readthrough process; DAP works exclusively with UGA PTC and tryptophan is the likely substituted amino acid in DAP-mediated readthrough [27]. The likely resultant missense mutations, p.(Arg261Trp) (AN1) and p.(Arg206Trp) (AN2), are both predicted pathogenic by in silico tools, hence although protein can be detected, it may likely non/dys-functional. Reports have shown that missense mutations can lead to milder phenotypes [3], however, this was not seen at a molecular level and may need in vivo studies to confirm this.

ABCG2 is a transient limbal epithelial stem cell marker, turned off when cells exit the stem cell state and start differentiation into corneal epithelial cells [39]. We hypothesize that ABCG2 increased levels in both AN iPSC-LESCs show that these cells may be unable to either switch off their proliferative status and/or trigger the differentiation process into corneal epithelial cells [40]. In parallel, we observe altered expression of neural crest marker *SOX10,* supporting the recent evidence that PAX6 has a role in neural crest-derived cells from the limbal niche [16,18]. Further differentiation of AN iPSC-LESCs into later stages as well as high throughput molecular characterisation of these cells would be important to not only understand the mechanisms behind PAX6-related LSCD but also to understand how iPSC-derived models compare to *in vivo* development and disease, particularly when dealing with such a regulatory-complex transcription factor like PAX6. Importantly, we observed variable efficiency in iPSC differentiation, particularly into LESCs; it is known that there can be substantial inter and intra-donor iPSC variability [35], which we tried to address by adding multiple control lines as well as clones for the same line; however, we acknowledge that the generation of PAX6 isogenic lines would be an important asset for proving the changes observed in patient cells derive exclusively from PAX6 defects.

Overall, patients with missense *PAX6* mutations tend to have milder ocular phenotypes [2,6]; in our recently published 86 aniridia patient cohort, patients with missense mutations have significantly

lower incidence of ARK, compared to patients with nonsense variants, who present with the highest ARK prevalence [3]. However, the nearly complete absence of aniridia patients with missense mutations located downstream of exon 7, coupled with the variable expressivity of the disease, makes it difficult to accurately predict the genotype-phenotype relationships. The closest reported missense variant to AN1 c.781C>T, p.(Arg261*) located in exon 10 (predicted homeodomain) was c.773T>C, p.(Phe258Ser); the patient presented with typical iris hypoplasia, and chorioretinal coloboma involving the optic disc, but indeed no description of aniridia related keratopathy (ARK) [48]. For AN2 c.607C>T/ p.(Arg203*) variant in exon 8, predicted in the linker region between both DNA-binding domains, the closest reported missense is p.(Arg208Gln), detected in a mid-twenties (at the time of evaluation) female described with mild symptoms, i.e. nystagmus, foveal hypoplasia and early cataract, but again, no ARK reported [49].

In this study we provide strong evidence supporting the repurposing of amlexanox as a putative therapeutic compound for aniridia patients with *PAX6* nonsense mutations. Our 3D optic cup models showed good tolerance to amlexanox, but in order to reduce off-target effects or systemic complications, topical formulations with a lower dose could be administered [50]. Further work on higher order *in vivo* models may be required to ascertain the optimal dose needed to induce optimal readthrough in aniridia patients. Interestingly, amlexanox has recently been shown to improve glucose levels and enhance liver fat loss in individuals with type II diabetes [51]. Hence, it could be beneficial to assess the effect of systemic amlexanox in aniridia patients, since recent reports show that aniridia patients commonly present with metabolic dysregulation leading to obesity and type II diabetes [3,52]. Therefore, we speculate that amlexanox might have ocular and wider systemic benefit in aniridia patients.

Lastly, this work provides further evidence that readthrough therapy seems to be a particularly promising therapeutic approach for aniridia, with previous *in vivo* models [12,13] and now patient-specific *in vitro* models showing positive pre-clinical outcomes. The advances in readthrough drug

development allied to more complex and representative human disease models will certainly allow for new compounds to be pushed into clinical trials for aniridia patients.

Materials and Methods

Ethics and clinical description

This study was approved by Moorfields Eye Hospital and the National Research Ethics Committee and was conducted in adherence to the tenets of the Declaration of Helsinki; informed written consent was obtained from all participants. 4-mm punch skin biopsies were obtained from the upper arm of a 6-year-old and a 10-year-old male aniridia patients with confirmed genotypes - *PAX6* c.781C>T, p.(Arg261*) (AN1), and c.607C>T/ p.(Arg203*) (AN2), respectively. The patient named AN1 was hypermetropic (right eye +6.00/-2.00x10 and left eye +6.00/-1.75x180) and their best corrected visual acuity was 0.74 LogMAR in each eye. Intraocular pressure was within normal range (18 mmHg in both eyes), no signs of glaucoma, cataracts or ARK, both cornea were clear. The patient does have complete iris and foveal hypoplasia. The patient AN2 was anisometropic (right eye plano and left eye -3.50/-3.00x160) and his best corrected visual acuity was RE 1.6 and LE 0.74 LogMAR. Intraocular pressure was RE 28 and LE 27 mmHg but no signs of glaucoma. He has a history of bilateral cataracts and has had lens extraction with RE being aphakic and LE receiving an intraocular lens implant. He has right ARK but the cornea is clear in LE. The patient does have complete iris and foveal hypoplasia

Induced Pluripotent Stem Cells (iPSC) generation and culture

AN patient iPSCs were generated using non-integrating episomal reprogramming of dermal fibroblasts extracted from a skin biopsy from the patient's arm, following established protocols [28,53]. A minimum of 2 clonal lines were expanded and characterised as previously described [29,53]. Control (WT) iPSCs used in this study were previously published [53]. The H9 embryonic stem cell line was obtained from WiCell (hPSCreg WAe009-A). All iPSC lines were maintained in mTESR Plus media

(StemCell Technologies, Canada) with 0.1% Pen/Strep on Matrigel-coated wells (1:100) (Corning, USA). For passaging, ReLESR (StemCell Technologies, Canada) was used for detaching and after 24h, iPSCs were fed daily with mTESR Plus until confluent.

iPSC-differentiation into 3D optic cups

Differentiation of iPSCs into 3D optic cups was performed based on published protocols [30,31]. Briefly, confluent iPSCs were detached with Accumax (ThermoFisher Scientific, USA) to single cell suspension and 3.6 million cells per well were plated onto Aggrewell400 plates (StemCell Technologies, Canada) (3,000 cells per microwell) in mTESR Plus with 10µM Y-27632 (Abcam), following manufacturer's instructions. After 48h, embryoid bodies (EBs) were collected and plated onto low attachment 60mm^2 plates in neural induction media (NIM) – DMEM/F12 (ThermoFisher Scientific), 20% knock-out serum replacement (KOSR) (ThermoFisher Scientific), 2% B27 (ThermoFisher Scientific), 1x Non-essential amino acids (NEAA; ThermoFisher Scientific), 1% Pen/Strep, 1xGlutamax (ThermoFisher Scientific) and 5ng/mL IGF-1 (Sigma-Aldrich) – until day 7. On day 8, cells were cultured in NIM with 15% KOSR and finally with 10% KOSR from day 11 until day 35 (Figure 1B).

iPSC differentiation into LESCs

Differentiation of iPSCs into LESCs was done following the protocol from Hongisto et al, with small adjustments [34]. Confluent iPSCs (~90/95%) were detached using ReLESR and clumps resuspended in mTESR Plus with 10µM Y-27632. Cell clumps were transferred into non-coated (petri) dishes and incubated O/N to allow the formation of EBs (Day 0). After 48h (Day 2), EBs were carefully washed with DPBS and resuspended in SM media (KnockOut DMEM supplemented with 15% xeno-free serum replacement, 2mM L-glutamine, 0.1mM 2-mercaptoethanol, 1% non-essential amino acids, and 50U/mL penicillin-streptomycin) supplemented with 10µM SB-505124 (Sigma Aldrich, USA) and 50ng/mL bFGF (Peprotech, USA). Media was replaced with SM media supplemented with 25ng/mL BMP-4 (Peprotech, USA) on days 3 and 4. On day 5, EBs were

carefully plated into collagen IV-coated wells in a mix of CnT30 media (CellnTech, Switzerland) and SM media (3:1) and allowed to attach for 48h. From there on, media was changed with CnT30 every other day until collection on day 15 for RNA and protein analysis.

Dosing and compounds information

Dosing concentrations of amlexanox (Abcam) and 2,6-diaminopurine (DAP, Sigma-Aldrich) were based on previous publications [24,26,27]. Known TRIDs ataluren/ PTC124 (ApexBio Tech LLC) and G418 (Life Technologies) were used as positive readthrough controls at 40µM and 100µg/mL, respectively, according to previous publications from our group [25,44,54]. 3D optic cups were dosed with amlexanox 250µM or ataluren 40µM in NIM+10%KOSR from day 15 to 35 of differentiation, with media refreshed every other day. iPSC-LESCs were dosed from day 13 to 15 of differentiation in CnT-30 media, with media change after 24h. Amlexanox (100µM and 200µM), DAP (100µM and 200µM), Ataluren (40µM) and G418 (100µg/mL) were tested.

RNA extraction and RT-qPCR

For transcript analysis of 3D optic cups, RNA extraction was performed after pellets collection using the RNeasy Mini or Micro Kit (QIAGEN, Germany); iPSC-LESCs were harvested by adding 300µL of Lysis buffer (Zymo Research, USA) and cells collected using a cell scraper; RNA was extracted following instructions in the Quick-RNA™ MicroPrep Kit w/ Zymo-Spin™ IC Columns kit (Zymo Research).

cDNA was synthesized from 500ng RNA using High-Capacity RNA-to-cDNA Kit (Life Technologies). RT-qPCR was performed with 2x SYBR Green MasterMix (ThermoFisher Scientific, USA) on a StepOne Real-Time PCR system (Applied Biosystems, UK) or QuantStudio 6 Flex (Applied Biosystems, UK). Primers used for qPCR are listed in Table S1. Transcript levels were measured in duplicate and normalised to housekeeper genes *GAPDH or ACTB*. The relative expression of each target gene was calculated using the comparative C_T method.

439 ***Western blotting***

440 Samples were analysed by western blotting as described previously [25,55]. Cells were washed with
441 ice-cold PBS and total protein extract was prepared with RIPA buffer with 1x Halt ™ protease
442 inhibitor cocktail and Halt ™ phosphatase inhibitor (ThermoFisher Scientific, MA, USA) at a ratio of
443 5x106 cells/mL. 30µg protein for iPSC-derived optic cups or 15µg for iPSC-LESCs were loaded
444 onto 4-15% Mini-PROTEAN ® TGX ™ gels (BioRad Inc., CA, USA) and transferred to an Immun-
445 Blot™ PVDF membrane using a Trans-Blot® SD semi-dry transfer cell (BioRad Inc., CA, USA).
446 Membranes were blocked with 5% non-fat dry milk in PBST for 2h, incubated overnight at 4○C with
447 the following primary antibodies diluted in blocking buffer: PAX6 (1:2000, Covance); ABCG2
448 (1 :1000, SantaCruz) ; β-actin (1:5000, SigmaAldrich). Incubation with horseradish peroxidase
449 conjugated secondary antibody anti-mouse or rabbit 1:5000 (Applied Biosystems, UK) was done
450 for 2h at room temperature. Membranes were incubated with Clarity Western ECL Substrate
451 (BioRad Inc., CA, USA) and imaged using the ChemiDoc XRS™ Imaging System (BioRad Inc.,
452 CA, USA). Band intensities were quantified using the Fiji/ImageJ software (National Institutes of
453 Health, MD, USA).

454

455 ***Immunofluorescence and Imaging***

456 Day 35 iPSC-OCs were processed for immunohistochemistry analysis following the protocol from
457 Reichmann et al [56]. Slides were imaged using an EVOS FL system (ThermoFisher Scientific, USA)
458 and ZEISS LSM 700 or LSM 710 (ZEISS Research, Germany).

459

460 ***Statistical Analysis***

461 Statistical analysis was performed using GraphPad Prism 8.0 (GraphPad Software Inc., San Diego,
462 CA, USA). One-Way ANOVA with multiple comparisons was used for comparison studies, with
463 significance achieved with p value of ≤ 0.05 (*), ≤ 0.01 (**), ≤ 0.001 (***). All results are expressed
464 as mean ± SD, unless specified. Experiments were performed with n = 3 biological replicates,
465 except when specified.

Author Contributions: MM designed research and acquired funding; DLC, HS, JE, PH, performed research; JZ contributed with reagents and research design; DLC and MM analysed data; DLC wrote the first draft; DLC and MM edited the manuscript with input from all authors.

Acknowledgments: The authors would like to thank the patients and their families for donating skin samples. Funding for this work was obtained from Moorfields Eye Charity, Wellcome Trust (205174/Z/16/Z), Fight for Sight and Aniridia Network to MM; EJP-RD (JPRD20-135) and NWO Visitor Travel Grant (040.11.699) to JZ and DLC.

Declaration of Interests Statement: The authors declare no competing interests.

Data Availability Statement: Data sharing not applicable to this article as no datasets were generated or analysed during the current study.

Keywords: amlexanox; aniridia; eye development; iPSCs; limbal epithelial stem cells; organoids; PAX6 haploinsufficiency; translational readthrough

References

1. Moosajee, M., Hingorani, M., and Moore, A.T. (2018). PAX6-Related Aniridia. In GeneReviews(®), (Seattle (WA): University of Washington, Seattle).
2. Hingorani, M., Williamson, K.A., Moore, A.T., and van Heyningen, V. (2009). Detailed ophthalmologic evaluation of 43 individuals with PAX6 mutations. Investigative ophthalmology & visual science *50*, 2581-2590. 10.1167/iovs.08-2827.
3. Kit, V., Lima Cunha, D., Hagag, A.M., and Moosajee, M. (2021). Longitudinal genotype-phenotype analysis in 86 PAX6-related aniridia patients. JCI insight. 10.1172/jci.insight.148406.
4. Daruich, A., Duncan, M., Robert, M.P., Lagali, N., Semina, E.V., Aberdam, D., Ferrari, S., Romano, V., des Roziers, C.B., Benkortebi, R., et al. (2022). Congenital aniridia beyond black eyes: From phenotype and novel genetic mechanisms to innovative therapeutic approaches. Progress in retinal and eye research, 101133. 10.1016/j.preteyeres.2022.101133.

5. Latta, L., Figueiredo, F.C., Ashery-Padan, R., Collinson, J.M., Daniels, J., Ferrari, S., Szentmáry, N., Solá, S., Shalom-Feuerstein, R., Lako, M., et al. (2021). Pathophysiology of aniridia-associated keratopathy: Developmental aspects and unanswered questions. The ocular surface *22*, 245-266. 10.1016/j.jtos.2021.09.001.
6. Lagali, N., Wowra, B., Fries, F.N., Latta, L., Moslemani, K., Utheim, T.P., Wylegala, E., Seitz, B., and Käsmann-Kellner, B. (2020). PAX6 Mutational Status Determines Aniridia-Associated Keratopathy Phenotype. Ophthalmology *127*, 273-275. 10.1016/j.ophtha.2019.09.034.
7. Jordan, T., Hanson, I., Zaletayev, D., Hodgson, S., Prosser, J., Seawright, A., Hastie, N., and van Heyningen, V. (1992). The human PAX6 gene is mutated in two patients with aniridia. Nature genetics *1*, 328-332. 10.1038/ng0892-328.
8. Hill, R.E., Favor, J., Hogan, B.L., Ton, C.C., Saunders, G.F., Hanson, I.M., Prosser, J., Jordan, T., Hastie, N.D., and van Heyningen, V. (1991). Mouse small eye results from mutations in a paired-like homeobox-containing gene. Nature *354*, 522-525. 10.1038/354522a0.
9. Lima Cunha, D., Arno, G., Corton, M., and Moosajee, M. (2019). The Spectrum of PAX6 Mutations and Genotype-Phenotype Correlations in the Eye. Genes *10*. 10.3390/genes10121050.
10. Way, C.M., Lima Cunha, D., and Moosajee, M. (2020). Translational readthrough inducing drugs for the treatment of inherited retinal dystrophies. Expert Review of Ophthalmology *15*, 169-182. 10.1080/17469899.2020.1762489.
11. Richardson, R., Smart, M., Tracey-White, D., Webster, A.R., and Moosajee, M. (2017). Mechanism and evidence of nonsense suppression therapy for genetic eye disorders. Experimental eye research *155*, 24-37. 10.1016/j.exer.2017.01.001.
12. Gregory-Evans, C.Y., Wang, X., Wasan, K.M., Zhao, J., Metcalfe, A.L., and Gregory-Evans, K. (2014). Postnatal manipulation of Pax6 dosage reverses congenital tissue malformation defects. The Journal of clinical investigation *124*, 111-116. 10.1172/jci70462.
13. Wang, X., Gregory-Evans, K., Wasan, K.M., Sivak, O., Shan, X., and Gregory-Evans, C.Y. (2017). Efficacy of Postnatal In Vivo Nonsense Suppression Therapy in a Pax6 Mouse Model of Aniridia. Molecular therapy. Nucleic acids *7*, 417-428. 10.1016/j.omtn.2017.05.002.
14. Shaham, O., Menuchin, Y., Farhy, C., and Ashery-Padan, R. (2012). Pax6: a multi-level regulator of ocular development. Progress in retinal and eye research *31*, 351-376. 10.1016/j.preteyeres.2012.04.002.
15. Collinson, J.M., Chanas, S.A., Hill, R.E., and West, J.D. (2004). Corneal development, limbal stem cell function, and corneal epithelial cell migration in the Pax6(+/-) mouse. Investigative ophthalmology & visual science *45*, 1101-1108. 10.1167/iovs.03-1118.
16. Chen, S.Y., Cheng, A.M.S., Zhang, Y., Zhu, Y.T., He, H., Mahabole, M., and Tseng, S.C.G. (2019). Pax 6 Controls Neural Crest Potential of Limbal Niche Cells to Support Self-Renewal of Limbal Epithelial Stem Cells. Scientific reports *9*, 9763. 10.1038/s41598-019-45100-7.
17. Su, Z., Wang, J., Lai, Q., Zhao, H., and Hou, L. (2020). KIT ligand produced by limbal niche cells under control of SOX10 maintains limbal epithelial stem cell survival by activating the KIT/AKT signalling pathway. Journal of cellular and molecular medicine *24*, 12020-12031. 10.1111/jcmm.15830.

18. Takamiya, M., Stegmaier, J., Kobitski, A.Y., Schott, B., Weger, B.D., Margariti, D., Cereceda Delgado, A.R., Gourain, V., Scherr, T., Yang, L., et al. (2020). Pax6 organizes the anterior eye segment by guiding two distinct neural crest waves. PLoS genetics *16*, e1008774. 10.1371/journal.pgen.1008774.
19. Takahashi, K., Tanabe, K., Ohnuki, M., Narita, M., Ichisaka, T., Tomoda, K., and Yamanaka, S. (2007). Induction of pluripotent stem cells from adult human fibroblasts by defined factors. Cell *131*, 861-872. 10.1016/j.cell.2007.11.019.
20. Hata, M., Ikeda, H.O., Iwai, S., Iida, Y., Gotoh, N., Asaka, I., Ikeda, K., Isobe, Y., Hori, A., Nakagawa, S., et al. (2018). Reduction of lipid accumulation rescues Bietti's crystalline dystrophy phenotypes. Proceedings of the National Academy of Sciences of the United States of America *115*, 3936-3941. 10.1073/pnas.1717338115.
21. Lane, A., Jovanovic, K., Shortall, C., Ottaviani, D., Panes, A.B., Schwarz, N., Guarascio, R., Hayes, M.J., Palfi, A., Chadderton, N., et al. (2020). Modeling and Rescue of RP2 Retinitis Pigmentosa Using iPSC-Derived Retinal Organoids. Stem cell reports *15*, 67-79. 10.1016/j.stemcr.2020.05.007.
22. Ramsden, C.M., Nommiste, B., A, R.L., Carr, A.F., Powner, M.B., M, J.K.S., Chen, L.L., Muthiah, M.N., Webster, A.R., Moore, A.T., et al. (2017). Rescue of the MERTK phagocytic defect in a human iPSC disease model using translational read-through inducing drugs. Scientific reports *7*, 51. 10.1038/s41598-017-00142-7.
23. Greer, R.O., Jr., Lindenmuth, J.E., Juarez, T., and Khandwala, A. (1993). A double-blind study of topically applied 5% amlexanox in the treatment of aphthous ulcers. Journal of oral and maxillofacial surgery : official journal of the American Association of Oral and Maxillofacial Surgeons *51*, 243-248; discussion 248-249. 10.1016/s0278-2391(10)80164-8.
24. Atanasova, V.S., Jiang, Q., Prisco, M., Gruber, C., Piñón Hofbauer, J., Chen, M., Has, C., Bruckner-Tuderman, L., McGrath, J.A., Uitto, J., et al. (2017). Amlexanox Enhances Premature Termination Codon Read-Through in COL7A1 and Expression of Full Length Type VII Collagen: Potential Therapy for Recessive Dystrophic Epidermolysis Bullosa. The Journal of investigative dermatology *137*, 1842-1849. 10.1016/j.jid.2017.05.011.
25. Eintracht, J., Forsythe, E., May-Simera, H., and Moosajee, M. (2021). Translational readthrough of ciliopathy genes BBS2 and ALMS1 restores protein, ciliogenesis and function in patient fibroblasts. EBioMedicine *70*, 103515. 10.1016/j.ebiom.2021.103515.
26. Gonzalez-Hilarion, S., Beghyn, T., Jia, J., Debreuck, N., Berte, G., Mamchaoui, K., Mouly, V., Gruenert, D.C., Déprez, B., and Lejeune, F. (2012). Rescue of nonsense mutations by amlexanox in human cells. Orphanet journal of rare diseases *7*, 58. 10.1186/1750-1172-7-58.
27. Trzaska, C., Amand, S., Bailly, C., Leroy, C., Marchand, V., Duvernois-Berthet, E., Saliou, J.M., Benhabiles, H., Werkmeister, E., Chassat, T., et al. (2020). 2,6-Diaminopurine as a highly potent corrector of UGA nonsense mutations. Nature communications *11*, 1509. 10.1038/s41467-020-15140-z.
28. Parfitt, D.A., Lane, A., Ramsden, C.M., Carr, A.F., Munro, P.M., Jovanovic, K., Schwarz, N., Kanuga, N., Muthiah, M.N., Hull, S., et al. (2016). Identification and Correction of Mechanisms Underlying Inherited Blindness in Human iPSC-Derived Optic Cups. Cell stem cell *18*, 769-781. 10.1016/j.stem.2016.03.021.
29. Harding, P., Lima Cunha, D., Méjécase, C., Eintracht, J., Toualbi, L., Sarkar, H., and Moosajee, M. (2021). Generation of human iPSC line (UCLi013-A) from a patient with

microphthalmia and aniridia, carrying a heterozygous missense mutation c.372C>A p.(Asn124Lys) in PAX6. Stem cell research *51*, 102184. 10.1016/j.scr.2021.102184.

30. Mellough, C.B., Collin, J., Khazim, M., White, K., Sernagor, E., Steel, D.H., and Lako, M. (2015). IGF-1 Signaling Plays an Important Role in the Formation of Three-Dimensional Laminated Neural Retina and Other Ocular Structures From Human Embryonic Stem Cells. Stem cells (Dayton, Ohio) *33*, 2416-2430. 10.1002/stem.2023.
31. Eintracht, J., Harding, P., Lima Cunha, D., and Moosajee, M. (2022). Efficient embryoid-based method to improve generation of optic vesicles from human induced pluripotent stem cells. F1000Research *11*, 324. 10.12688/f1000research.108829.1.
32. Nakano, T., Ando, S., Takata, N., Kawada, M., Muguruma, K., Sekiguchi, K., Saito, K., Yonemura, S., Eiraku, M., and Sasai, Y. (2012). Self-formation of optic cups and storable stratified neural retina from human ESCs. Cell stem cell *10*, 771-785. 10.1016/j.stem.2012.05.009.
33. Zhong, X., Gutierrez, C., Xue, T., Hampton, C., Vergara, M.N., Cao, L.H., Peters, A., Park, T.S., Zambidis, E.T., Meyer, J.S., et al. (2014). Generation of three-dimensional retinal tissue with functional photoreceptors from human iPSCs. Nature communications *5*, 4047. 10.1038/ncomms5047.
34. Hongisto, H., Vattulainen, M., Ilmarinen, T., Mikhailova, A., and Skottman, H. (2018). Efficient and Scalable Directed Differentiation of Clinically Compatible Corneal Limbal Epithelial Stem Cells from Human Pluripotent Stem Cells. Journal of visualized experiments : JoVE. 10.3791/58279.
35. Beekhuis-Hoekstra, S.D., Watanabe, K., Werme, J., de Leeuw, C.A., Paliukhovich, I., Li, K.W., Koopmans, F., Smit, A.B., Posthuma, D., and Heine, V.M. (2021). Systematic assessment of variability in the proteome of iPSC derivatives. Stem cell research *56*, 102512. 10.1016/j.scr.2021.102512.
36. Rabiee, B., Anwar, K.N., Shen, X., Putra, I., Liu, M., Jung, R., Afsharkhamseh, N., Rosenblatt, M.I., Fishman, G.A., Liu, X., et al. (2020). Gene dosage manipulation alleviates manifestations of hereditary PAX6 haploinsufficiency in mice. Science translational medicine *12*. 10.1126/scitranslmed.aaz4894.
37. Ouyang, J., Shen, Y.C., Yeh, L.K., Li, W., Coyle, B.M., Liu, C.Y., and Fini, M.E. (2006). Pax6 overexpression suppresses cell proliferation and retards the cell cycle in corneal epithelial cells. Investigative ophthalmology & visual science *47*, 2397-2407. 10.1167/iovs.05-1083.
38. Hancock, H.A., Guidry, C., Read, R.W., Ready, E.L., and Kraft, T.W. (2005). Acute aminoglycoside retinal toxicity in vivo and in vitro. Investigative ophthalmology & visual science *46*, 4804-4808. 10.1167/iovs.05-0604.
39. Vattulainen, M., Ilmarinen, T., Koivusalo, L., Viiri, K., Hongisto, H., and Skottman, H. (2019). Modulation of Wnt/BMP pathways during corneal differentiation of hPSC maintains ABCG2-positive LSC population that demonstrates increased regenerative potential. Stem cell research & therapy *10*, 236. 10.1186/s13287-019-1354-2.
40. Latta, L., Nordström, K., Stachon, T., Langenbucher, A., Fries, F.N., Szentmáry, N., Seitz, B., and Käsmann-Kellner, B. (2019). Expression of retinoic acid signaling components ADH7 and ALDH1A1 is reduced in aniridia limbal epithelial cells and a siRNA primary cell based aniridia model. Experimental eye research *179*, 8-17. 10.1016/j.exer.2018.10.002.
41. Tzoulaki, I., White, I.M., and Hanson, I.M. (2005). PAX6 mutations: genotype-phenotype correlations. BMC genetics *6*, 27. 10.1186/1471-2156-6-27.

42. Wawrocka, A., and Krawczynski, M.R. (2018). The genetics of aniridia - simple things become complicated. Journal of applied genetics *59*, 151-159. 10.1007/s13353-017-0426-1.
43. Marquardt, T., Ashery-Padan, R., Andrejewski, N., Scardigli, R., Guillemot, F., and Gruss, P. (2001). Pax6 is required for the multipotent state of retinal progenitor cells. Cell *105*, 43-55. 10.1016/s0092-8674(01)00295-1.
44. Sarkar, H., Mitsios, A., Smart, M., Skinner, J., Welch, A.A., Kalatzis, V., Coffey, P.J., Dubis, A.M., Webster, A.R., and Moosajee, M. (2019). Nonsense-mediated mRNA decay efficiency varies in choroideremia providing a target to boost small molecule therapeutics. Human molecular genetics *28*, 1865-1871. 10.1093/hmg/ddz028.
45. Zetoune, A.B., Fontanière, S., Magnin, D., Anczuków, O., Buisson, M., Zhang, C.X., and Mazoyer, S. (2008). Comparison of nonsense-mediated mRNA decay efficiency in various murine tissues. BMC genetics *9*, 83. 10.1186/1471-2156-9-83.
46. Yu, F., Zhang, W., Yan, C., Yan, D., Zhou, M., Chen, J., Zhao, X., Zhu, A., Zhou, J., Liu, H., et al. (2020). PAX6, modified by SUMOylation, plays a protective role in corneal endothelial injury. Cell death & disease *11*, 683. 10.1038/s41419-020-02848-5.
47. Tsui, S., Wang, J., Wang, L., Dai, W., and Lu, L. (2016). CTCF-Mediated and Pax6-Associated Gene Expression in Corneal Epithelial Cell-Specific Differentiation. PloS one *11*, e0162071. 10.1371/journal.pone.0162071.
48. Azuma, N., Yamaguchi, Y., Handa, H., Tadokoro, K., Asaka, A., Kawase, E., and Yamada, M. (2003). Mutations of the PAX6 gene detected in patients with a variety of optic-nerve malformations. American journal of human genetics *72*, 1565-1570. 10.1086/375555.
49. Grønskov, K., Rosenberg, T., Sand, A., and Brøndum-Nielsen, K. (1999). Mutational analysis of PAX6: 16 novel mutations including 5 missense mutations with a mild aniridia phenotype. European journal of human genetics : EJHG *7*, 274-286. 10.1038/sj.ejhg.5200308.
50. Woodley, D.T., Cogan, J., Hou, Y., Lyu, C., Marinkovich, M.P., Keene, D., and Chen, M. (2017). Gentamicin induces functional type VII collagen in recessive dystrophic epidermolysis bullosa patients. The Journal of clinical investigation *127*, 3028-3038. 10.1172/jci92707.
51. Oral, E.A., Reilly, S.M., Gomez, A.V., Meral, R., Butz, L., Ajluni, N., Chenevert, T.L., Korytnaya, E., Neidert, A.H., Hench, R., et al. (2017). Inhibition of IKKε and TBK1 Improves Glucose Control in a Subset of Patients with Type 2 Diabetes. Cell metabolism *26*, 157-170.e157. 10.1016/j.cmet.2017.06.006.
52. Netland, P.A., Scott, M.L., Boyle, J.W.t., and Lauderdale, J.D. (2011). Ocular and systemic findings in a survey of aniridia subjects. Journal of AAPOS : the official publication of the American Association for Pediatric Ophthalmology and Strabismus *15*, 562-566. 10.1016/j.jaapos.2011.07.009.
53. Méjécase, C., Harding, P., Sarkar, H., Eintracht, J., Lima Cunha, D., Toualbi, L., and Moosajee, M. (2020). Generation of two human control iPS cell lines (UCLi016-A and UCLi017-A) from healthy donors with no known ocular conditions. Stem cell research *49*, 102113. 10.1016/j.scr.2020.102113.
54. Torriano, S., Erkilic, N., Baux, D., Cereso, N., De Luca, V., Meunier, I., Moosajee, M., Roux, A.F., Hamel, C.P., and Kalatzis, V. (2018). The effect of PTC124 on choroideremia fibroblasts and iPSC-derived RPE raises considerations for therapy. Scientific reports *8*, 8234. 10.1038/s41598-018-26481-7.

55. Moosajee, M., Tracey-White, D., Smart, M., Weetall, M., Torriano, S., Kalatzis, V., da Cruz, L., Coffey, P., Webster, A.R., and Welch, E. (2016). Functional rescue of REP1 following treatment with PTC124 and novel derivative PTC-414 in human choroideremia fibroblasts and the nonsense-mediated zebrafish model. Human molecular genetics *25*, 3416-3431. 10.1093/hmg/ddw184.
56. Reichman, S., and Goureau, O. (2016). Production of Retinal Cells from Confluent Human iPS Cells. Methods in molecular biology (Clifton, N.J.) *1357*, 339-351. 10.1007/7651_2014_143.

List of Figure Captions

Figure 1. Generation of aniridia iPSC-derived optic cups. (A) Direct sequencing of *PAX6* exon 10 showing the heterozygous nonsense c.781C>T change in AN1 patient iPSCs. This variant was not detected in control lines. **(B)** Schematic representation of the differentiation strategy of control WT1 and WT2, and patient-derived AN1 iPSCs into 3D optic cups (35 days). Data from WT1 control line is included as an example. Dosing experiments with TRIDs were performed from day 15 onwards. **(C,D)** RT-qPCR transcript analysis of eye field transcription factors *RAX* and *PAX6* during 35 days of differentiation in control (WT1, blue) and aniridia (AN,1 red) iPSCs. Values were normalised to day 0 and to internal housekeeping gene *GAPDH*. Data represent means and SD of n=3 biological replicates. **(E)** RT-PCR followed by Sanger sequencing of *PAX6* cDNA from day 35 WT1 and AN1 iPSC-OCs. The mutated allele c.781C>T can be seen in AN1 but not in WT1 iPSC-OCs. **(F)** PAX6 protein analysis detected by western blot in WT and AN1 iPSC-OCs from day 25 to 35 of differentiation (5-day intervals). PAX6/β-actin ratio was normalised to WT1. n=3 (** $p<0.01$, t-test analysis). **(G)** Immunohistochemical analysis of WT1 and AN iPSC-derived optic cups showing positive staining of PAX6 (green), as well as markers for optic cup domains: VSX2 indicating the neural retina (red, upper panel) and MITF indicating retinal pigmented epithelium (RPE) (red, lower panel). DAPI staining (blue) shows cell nuclei. Scale bar 100µm**.** .

Figure 2. Characterisation of iPSC-derived limbal epithelial stem cell (LESC) from 2 aniridia patients. (A) Schematic representation of differentiation protocol used in this study, based on [34]. **(B)** RT-qPCR transcript analysis of LESC markers Δ*NP63α* (measured with 2 primer pairs), *KRT14* and *ABCG2* in 2 aniridia (AN1 and AN2) and 2 independent control (WT1 and WT2) iPSC lines, showing limbal commitment by day 15 of differentiation. **(C)** RT-qPCR transcript analysis of *PAX6* showed no significant difference in expression in AN vs WT lines. Values were normalised to day 0 and to internal housekeeper gene *GAPDH*. Data represent means and SD of n=3 biological replicates. **(D)** Protein analysis detected by western blot revealed decreased PAX6 levels between AN1 and AN2 versus WT (WT2 included as an example) samples on day 10 and being statistical significant on day 15 of differentiation. PAX6/β-actin ratio was normalised to control (WT). n=3 (* p<0.05, t-test analysis).

Figure 3. Effect of Translational readthrough inducing drugs (TRIDs) in day 35 aniridia iPSC-derived optic cups (iPSC-OCs). (A) Bright-field images of control (WT), untreated aniridia (AN1 UT), amlexanox-treated aniridia (AN1 Amlex) and ataluren-treated aniridia (AN1 Atal) iPSC-OCs. Scale bar 100µm. **(B)** Quantification of PAX6 protein in treated vs untreated AN1 iPSC-OCs (red bars). PAX6/β-actin ratio was normalised to control (WT, blue bar). (*, p<0.05; **, p<0.01, one-way ANOVA). Data represent means and SD of at least n=3 biological replicates. **(C)** Immunofluorescence analysis on day 35 of differentiation, showing PAX6 staining (green) and DAPI (blue) in control (WT), untreated aniridia (AN1 UT), amlexanox-treated aniridia (AN1 Amlex) and ataluren-treated aniridia (AN1 Atal) iPSC-OCs. Scale bar 100µm. **(D)** RT-qPCR transcript analysis of neural retina marker *VSX2* in WT (blue bar) and AN1 UT, AN1 Amlex and AN1 Atal samples (red bars). (*, p<0.05; **, p<0.01, one-way ANOVA). **(E)** Immunohistochemical analysis showing VSX2 staining in WT, AN1 UT, amlexanox- and ataluren-treated iPSC-OCs. DAPI staining in blue, Scale bar 100µm. Red bright spots visible in WT and AN1 Amlex are background staining. **(F)** RT-qPCR transcript analysis of proliferation marker *MKi67* in WT (blue bar) and AN1 UT, AN1 Amlex and AN1 Atal samples (red bars) (***, p<0.001, one-way ANOVA). **(D, F)** Values were

normalised to WT and to internal housekeeper gene *GAPDH*. Data represent means and SD of at least n=3 biological replicates.

Figure 4. TRIDs rescue PAX6 expression in AN1 iPSC-derived LESCs. (A) Quantification of PAX6 protein in untreated (UT) AN1 iPSC-LESCs versus amlexanox-, DAP- and ataluren-treated AN1 iPSC-LESCs (red bars). PAX6/ β-actin ratio was normalised to control (WT, blue bar). Values in x axis refer to compounds concentrations in µM. (*, p<0.05; ***, p<0.001; ****, p<0.0001; one-way ANOVA). Data represent means and SD of at least n=3 biological replicates. (B) Quantification of ABCG2 protein detected by western blot in WT (blue bar), AN1 untreated and amlexanox-, DAP- and ataluren-treated AN1 iPSC-LESCs (red bars). PAX6/β-actin ratio was normalised to control (WT). Data represent means and SD of n=3 biological replicates (*, p<0.05, one-way ANOVA). **(C)** Relative expression of *SOX9* transcripts in WT1 and WT2 and AN1 iPSC-LESCs. Significance was calculated using multiple t-test between AN1 and both WT lines. **(D)** RT-qPCR transcript analysis of neural crest marker *SOX10* in WT (blue bar) and AN1 UT, AN1 Amlex and AN1 Atal samples (red bars). (***, p<0.001, **, p<0.01; one-way ANOVA). **(C, D)** Values were normalised to WT and to internal housekeeper gene *GAPDH*. Data represent means and SD of at least n=3 biological replicates.

Figure 5. TRIDs show trend improvement in PAX6 expression in AN2 iPSC-derived LESCs. (A) Quantification of PAX6 protein in untreated (UT) AN2 iPSC-LESCs versus amlexanox-, DAP- and ataluren-treated AN2 iPSC-LESCs (green bars). PAX6/β-actin ratio was normalised to control (WT, blue bar). Values in x axis refer to compounds concentrations in µM. (*, p<0.05; **, p<0.01; one-way ANOVA). Data represent means and SD of at least n=3 biological replicates. (B) Quantification of ABCG2 protein detected by western blot in WT (blue bar), AN2 untreated and amlexanox-, DAP- and ataluren-treated AN2 iPSC-LESCs (green bars). Values in x axis refer to compounds concentrations in µM. PAX6/ β-actin ratio was normalised to control (WT). Data represent means and SD of n=3 biological replicates (*, p<0.05, one-way ANOVA). **(C)** Relative

763 expression of *SOX9* transcripts in WT1 and WT2 and AN2 iPSC-LESCs. Significance was
764 calculated using multiple t-test between AN and both WT lines. **(D)** RT-qPCR transcript analysis of
765 neural crest marker *SOX10* in WT (blue bar) and AN UT, AN Amlex and AN Atal samples (green
766 bars). (***, p<0.001, **, p<0.01; one-way ANOVA). **(C, D)** Values were normalised to WT and to
767 internal housekeeper gene *GAPDH*. Data represent means and SD of at least n=3 biological
768 replicates.

769

770

771

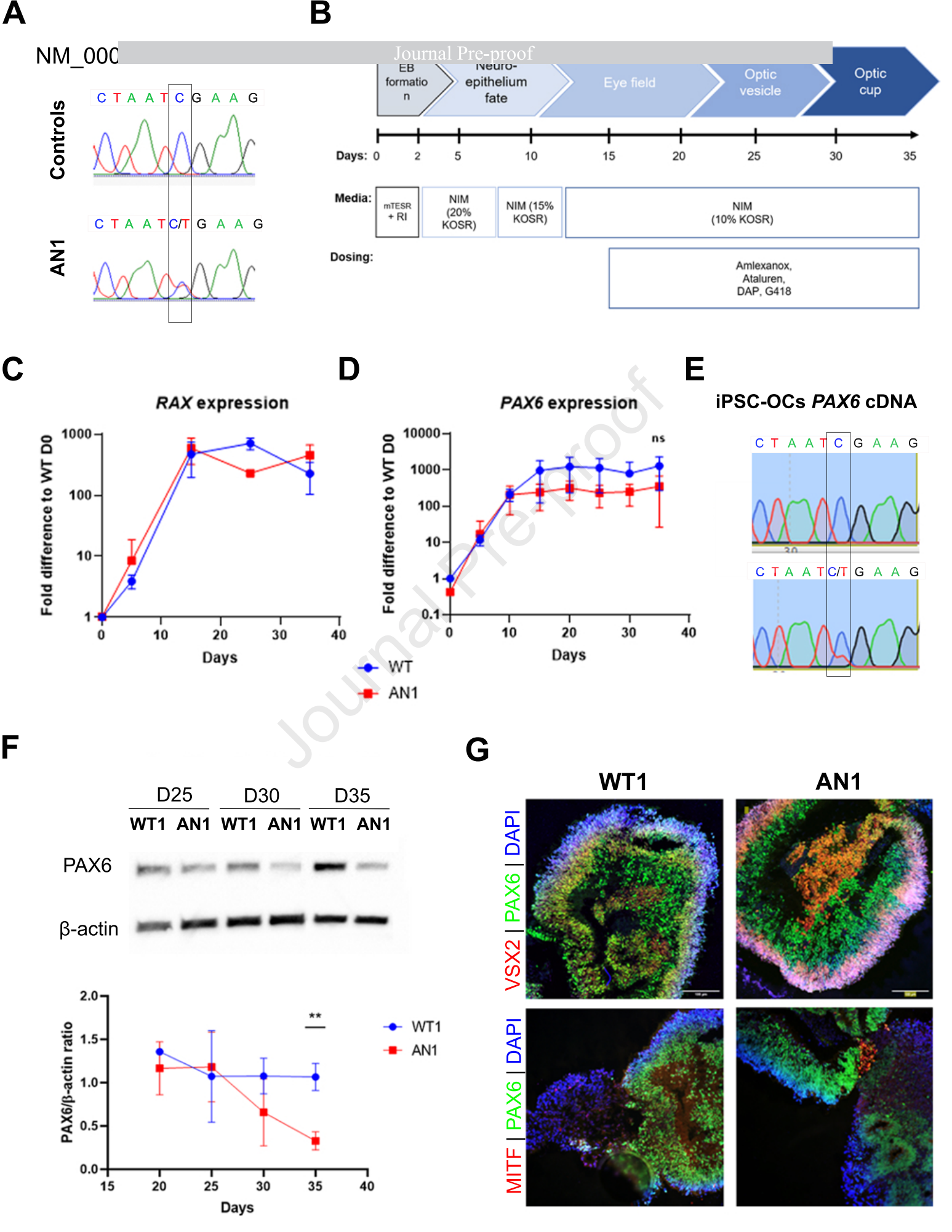

A

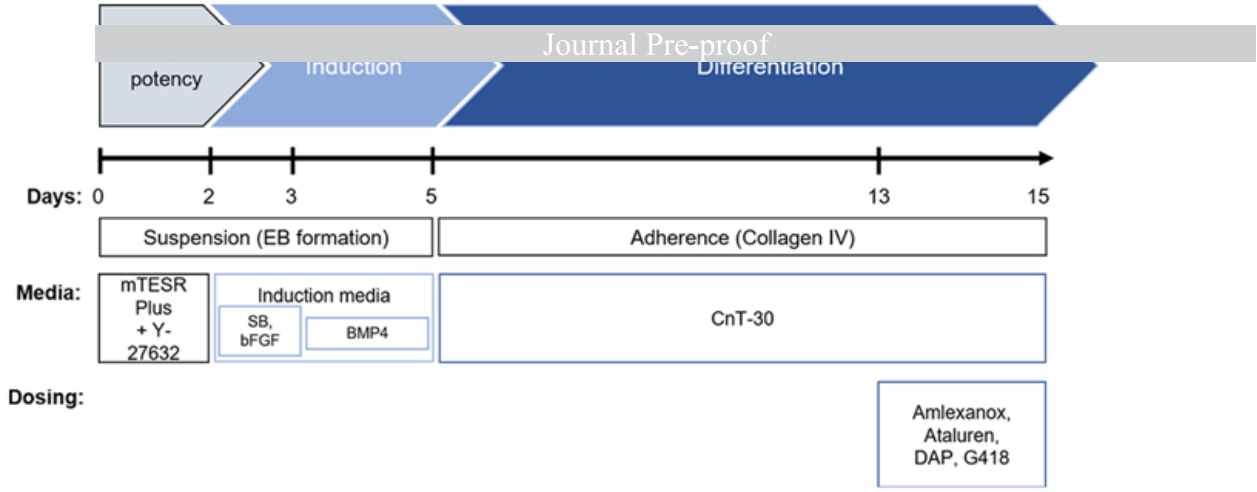

B

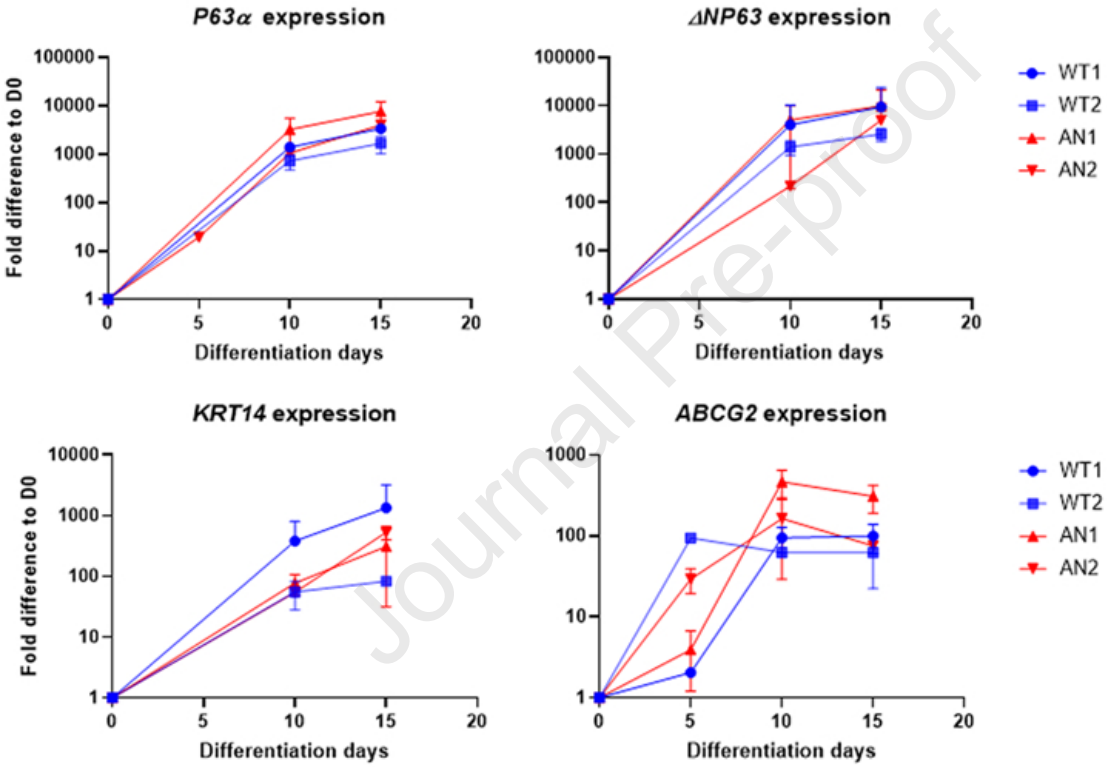

C

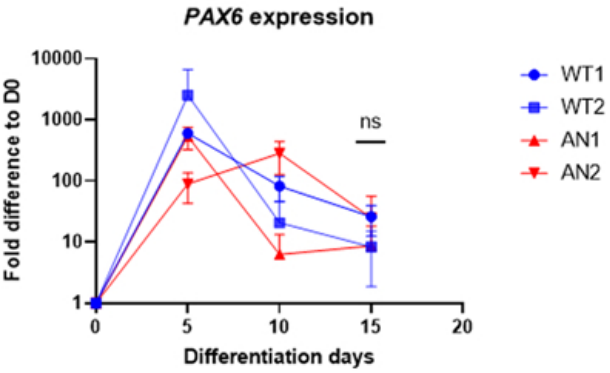

D

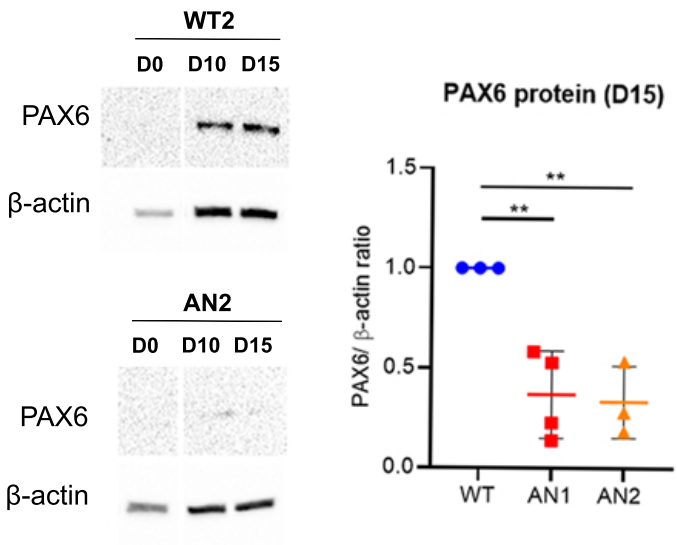

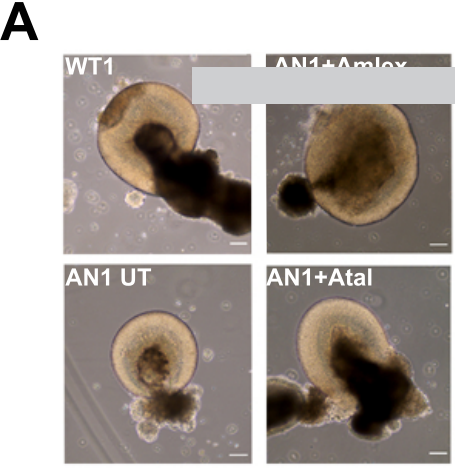

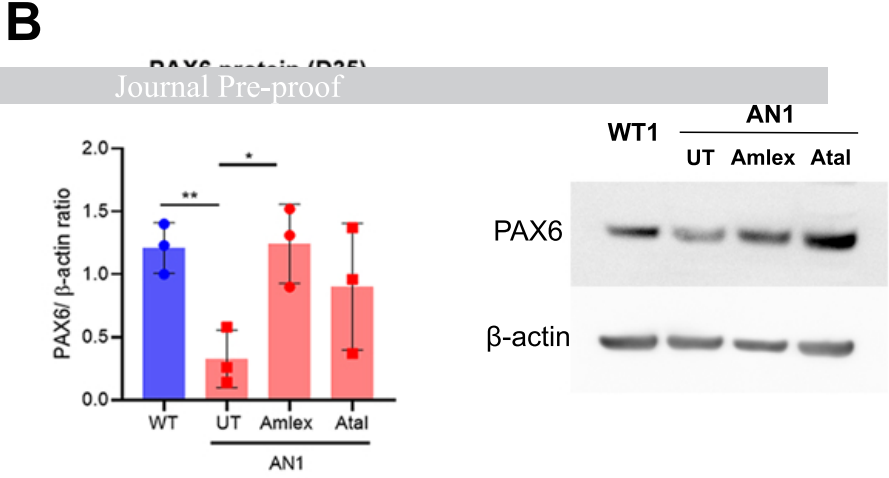

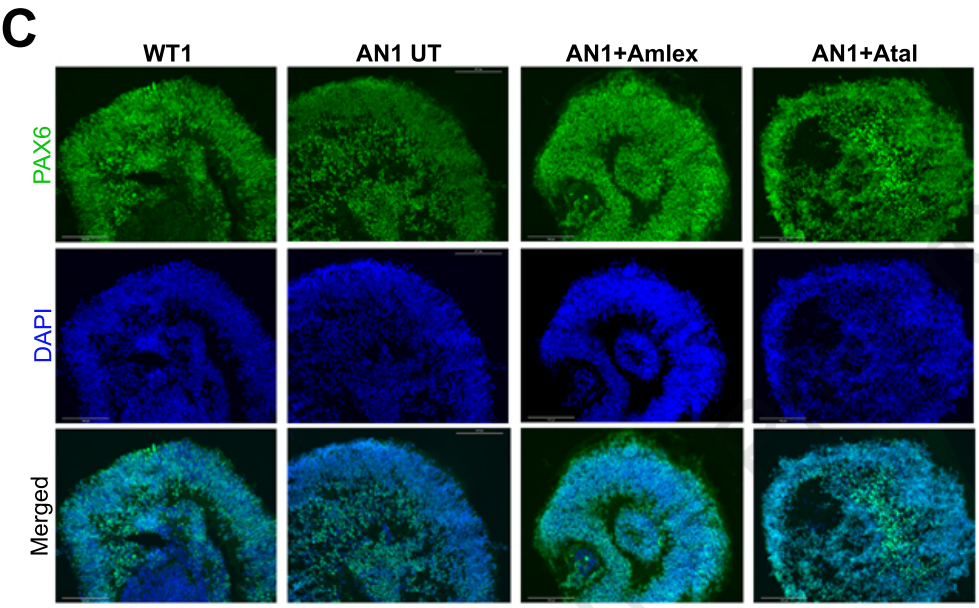

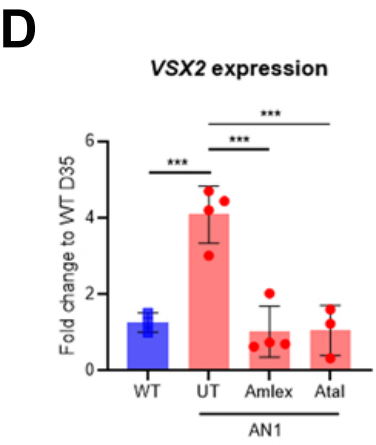

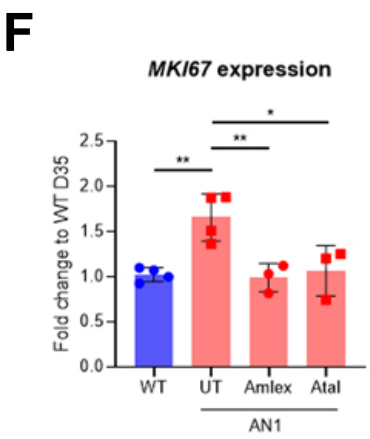

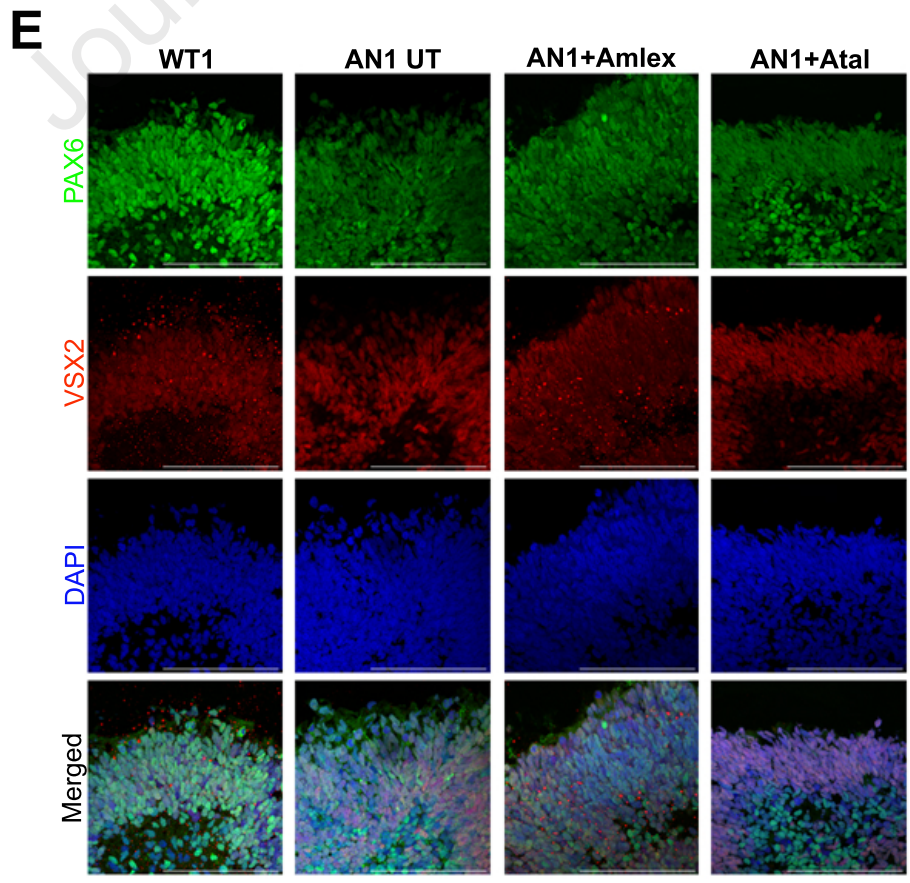

A

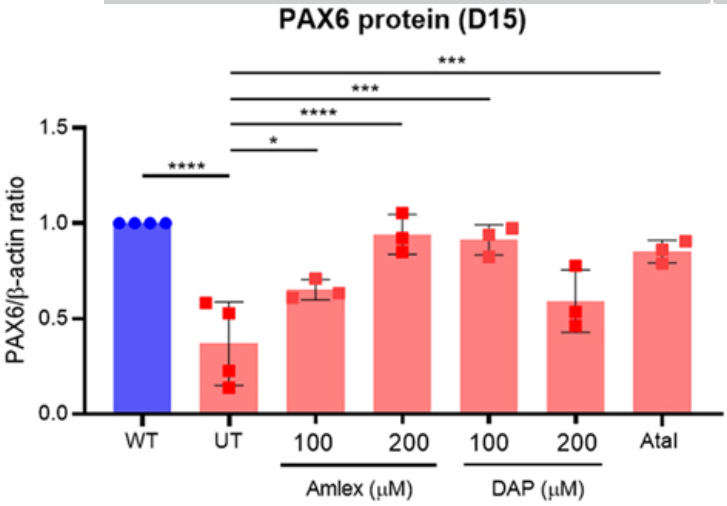

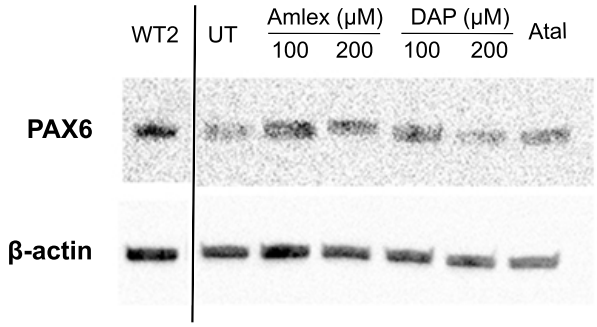

B

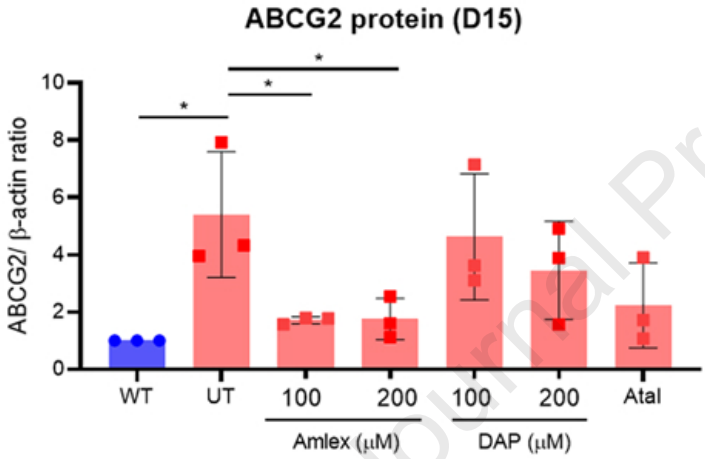

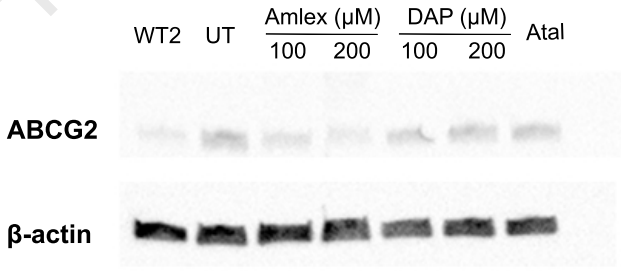

C

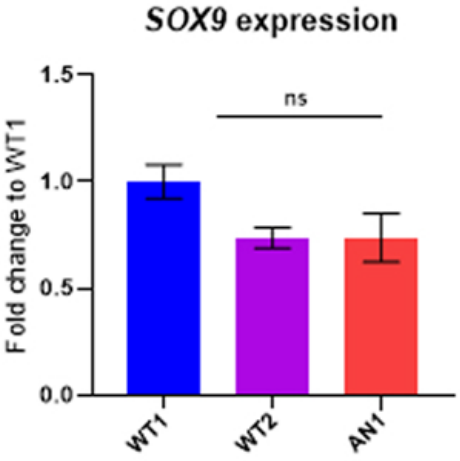

D

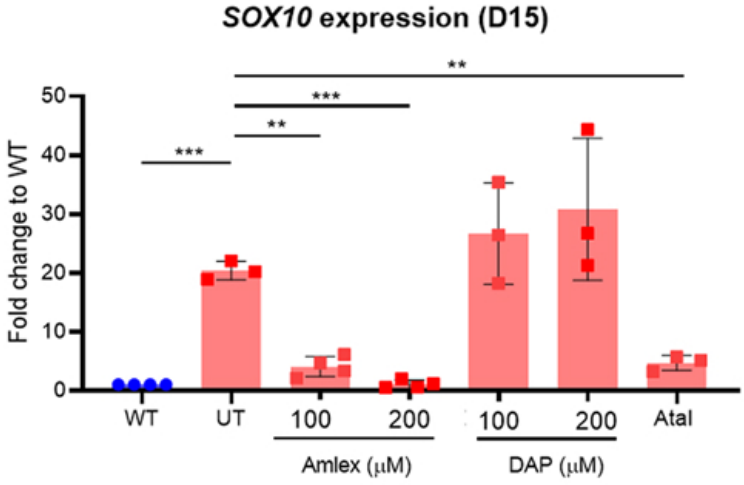

A

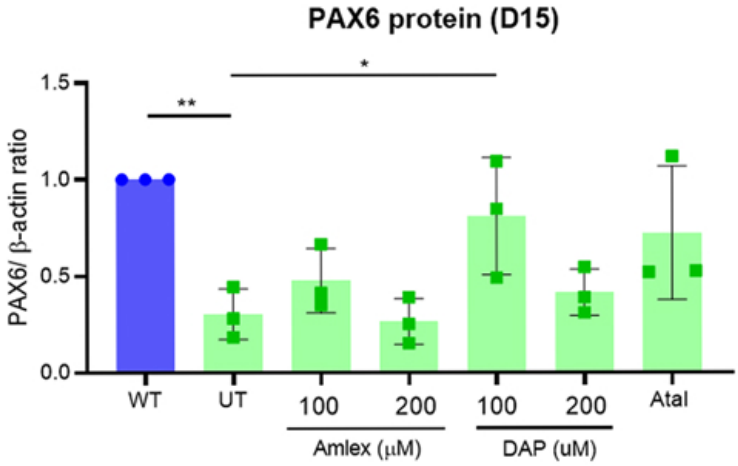

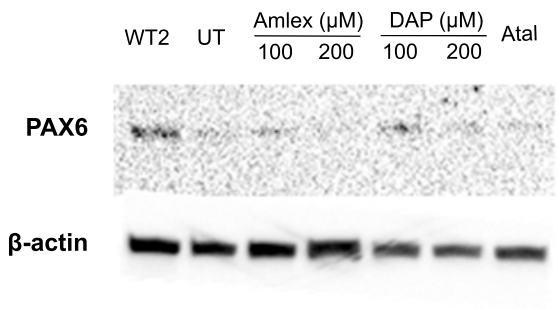

B

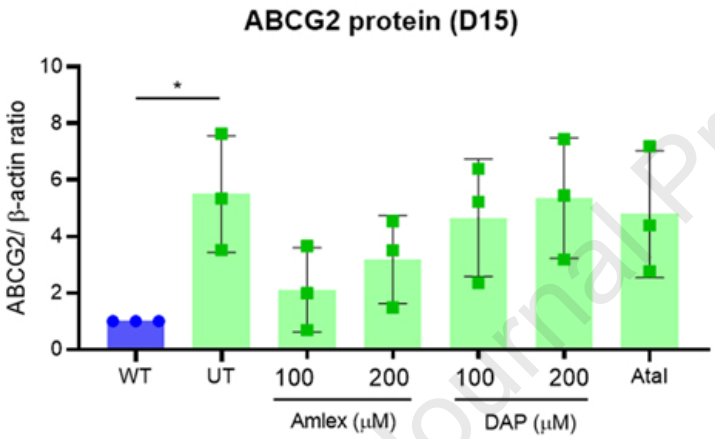

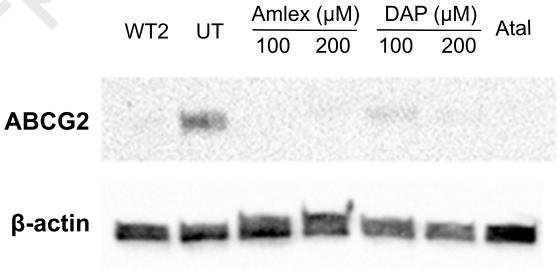

C

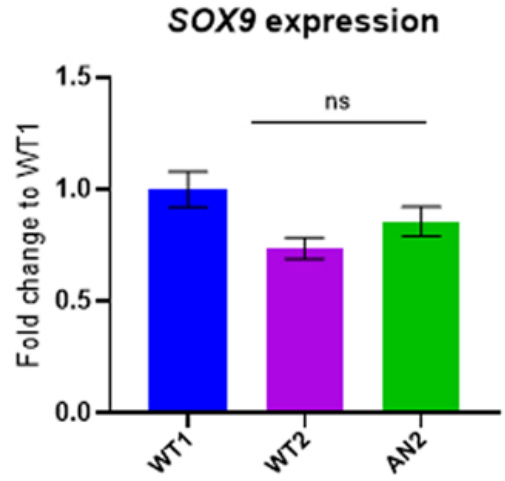

D

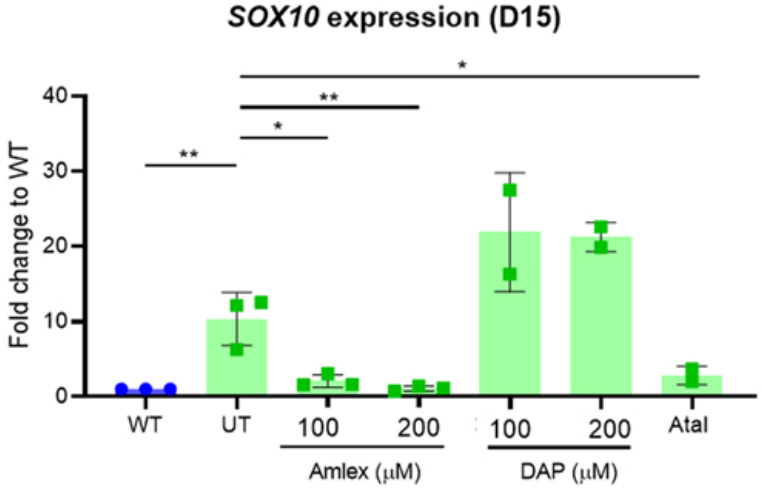

Moosajee and colleagues present a proof of concept study supporting the use of readthrough drug amlexanox as a new therapeutic approach for aniridia patients carrying nonsense *PAX6* mutations. The authors show this compound increases full-length PAX6 levels in novel patient induced pluripotent stem cell-derived retinal and corneal models.